

# Targeting Specific PDZ Domains of PSD-95: Structural Basis for Enhanced Affinity and Enzymatic Stability of a Cyclic Peptide

Andrea Piserchio,<sup>1</sup> Gregory D. Salinas,<sup>2</sup> Tao Li,<sup>3</sup>  
John Marshall,<sup>2</sup> Mark R. Spaller,<sup>3,\*</sup>  
and Dale F. Mierke<sup>1,2,\*</sup>

<sup>1</sup>Department of Chemistry

<sup>2</sup>Department of Molecular Pharmacology

Division of Biology & Medicine

Brown University

Providence, Rhode Island 02912

<sup>3</sup>Department of Chemistry

Wayne State University

Detroit, Michigan 48202

## Summary

A cyclic peptide, Tyr-Lys-c[-Lys-Thr-Glu( $\beta$ Ala)-]-Val, incorporating a  $\beta$ -Ala lactam side chain linker and designed to target the PDZ domains of the postsynaptic density protein 95 (PSD-95), has been synthesized and structurally characterized by NMR while free and bound to the PDZ1 domain of PSD-95. While bound, the lactam linker of the peptide makes a number of unique contacts outside the canonical PDZ binding motif, providing a novel target for PDZ-domain specificity as well as producing a 10-fold enhancement in binding affinity. Additionally, the cyclization greatly enhances the enzymatic stability, increasing the duration that the peptide inhibits the association between PSD-95 and glutamate receptors, effectively inhibiting the clustering of kainate receptors for over 14 hr after application. Highly specific regulation of kainate receptor action may provide a novel route for treatment of drug addiction and epilepsy.

## Introduction

The postsynaptic density protein 95 (PSD-95), also known as synapse associated protein-90 (SAP-90), regulates signaling in glutamatergic neurons by acting as a molecular scaffold for the formation of protein complexes localized at the postsynaptic density of dendritic spines. Each of the five domains of PSD-95 [1-3]—three PDZ, an SH3, and an inactive guanylate kinase domain—can individually (or in tandem) interact with several targets, including ion channel receptors, adhesion and cytoskeleton proteins, and proteins involved in intracellular signaling. In particular, the three PDZ domains are important in the modulation of these protein-protein interactions.

The PDZ domains of PSD-95 share high sequence homology and have similar three-dimensional structures [4-6] resembling the canonical PDZ conformation consisting of an antiparallel  $\beta$  sandwich formed by two  $\alpha$  helices and six  $\beta$  strands. The binding pocket, located between the second  $\beta$  strand and the first  $\alpha$  helix, binds the C termini of proteins sharing the (S/T)-X-(V/I/L)-

COOH consensus motif (where X stands for any amino acid). The binding cleft or pocket of the PDZ domain is shallow and nondescript, consistent with the short-lived, transient interactions aimed to bring proteins together to facilitate signaling and then rapidly disperse.

Although sequentially and structurally similar, the PDZ domains of PSD-95 in fact exhibit distinct preferences for binding partners. Unfortunately, the origin of the PDZ domain specificity is still not well understood. Binding studies based on peptide libraries have shown that all of the last five C-terminal residues actively contribute to the interaction. Indeed, the X-ray analysis of the complex of PDZ3 with the C terminus of CRIPT provides structural information for only the last five residues of CRIPT [4]. NMR studies of PDZ1 and PDZ2 of PSD-95 [5, 6] have shown that the loop between the second and third  $\beta$  strands is affected by ligand association, suggesting that the loop plays an important role in the binding process and maybe in ligand specificity.

As a first step to increase both the binding and specificity of the peptide ligands for the PDZ domains of the PSD-95, we have designed, synthesized, and examined the structural features of a novel cyclic analog while bound to the PDZ1 domain of PSD-95. The resulting structural features indicate that the side chain to side chain lactam bridge stabilizes the extended structure required for binding, leading to a 10-fold enhancement in binding and affords a mechanism for enhanced PDZ specificity. Additionally, the cyclic peptide displays a longer duration of biological function, a fact of diminished enzymatic degradation.

## Results and Discussion

### Peptide Design

As part of a program to develop novel ligands for the PDZ domain, a bridged cyclic peptide scaffold was designed that allows for systematic variation in ring size [7]. The cyclic peptide was designed based on the six C-terminal residues of CRIPT, where Ser<sup>-1</sup> and Gln<sup>-3</sup> (starting from the C terminus, Val is indicated as position 0) have been replaced by glutamic acid and lysine, respectively. These two side chains were then cyclized using  $\beta$ -alanine as a linker (Figure 1). We previously have shown that the C-terminal peptide of CRIPT binds to PDZ1 of PSD-95 with a dissociation constant of 10  $\mu$ M [5]. The cyclization was designed to stabilize an extended conformation of the peptide as observed for PDZ3 bound form of CRIPT. Indeed, the NMR-derived structures of the free cyclic peptide revealed limited conformations (in comparison to linear peptides) with similar features to the structure while bound to PDZ1. Based on the high-resolution structure of the peptide alone in aqueous solution (data not shown), the average distance between the C $\alpha$  of K<sup>-3</sup> and Val<sup>0</sup> is 9.2 Å, only 0.4 Å shorter than while associated with PDZ1.

### Structure of the Peptide/PDZ1 Complex

In the presence of PDZ1, the resonances of the peptide undergo frequency shifts and line broadening, indicating

\*Correspondence: dale\_mierke@brown.edu; mspaller@chem.wayne.edu

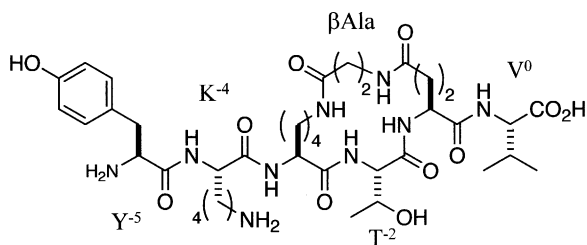


Figure 1. Design of Cyclic Ligand

Structural formula of the cyclic lactam containing peptide, Tyr-Lys-c[-Lys-Thr-Glu( $\beta$ Ala)-]-Val, examined here.

a fast exchange regime between the bound and unbound forms. From a careful titration of PDZ1 with the peptide, a dissociation constant of 1  $\mu$ M is calculated for the cyclic peptide (Figure 2). Based on numerous NOEs (Table 1), the peptide binds to PDZ1 in the groove between the  $\beta$ 2 strand and  $\alpha$ 2 helix as previously reported for other peptides [5] (Figure 3). The peptide backbone encompassing residues Val<sup>0</sup> and Thr<sup>-2</sup> forms an additional antiparallel  $\beta$  strand interacting with Phe<sup>77</sup>, Ser<sup>78</sup>, and Ile<sup>79</sup> of the  $\beta$ 2 strand of PDZ1 (Figure 4). The chemical shift perturbations of the backbone resonances of PDZ1 upon ligand titration are consistent with the NOE-derived structure: the <sup>1</sup>H<sup>15</sup>N amide resonances shift toward lower field, indicating an increase in hydrogen bond content, while the <sup>13</sup>C<sup>1</sup>H $\alpha$  chemical shifts move toward more accentuated  $\beta$  sheet values.

The side chain of Val<sup>0</sup> is in a hydrophobic binding pocket formed by Leu<sup>75</sup>, Phe<sup>77</sup>, Ile<sup>78</sup>, and Leu<sup>137</sup>. The C-terminal carboxylic acid is surrounded by the amide groups of Leu<sup>75</sup>, Gly<sup>76</sup>, and Phe<sup>77</sup>, whose NMR resonances are strongly shifted toward lower field, consistent with formation of hydrogen bonds. The hydroxyl group of Thr<sup>-2</sup> hydrogen bonds the imidazole moiety of His<sup>130</sup>, while the methyl group makes hydrophobic contacts with Ile<sup>79</sup> on the  $\beta$ 2 strand and with Val<sup>134</sup> on the helix side.

Outside the ligand binding pocket, the perturbation of NMR signals is generally diminished, with the exception of residues of the  $\beta$ 2- $\beta$ 3 loop. The involvement of this loop in the ligand recognition process represents an important differentiation of ligand binding to PDZ1 and PDZ3 of PSD-95. In the PDZ3/CRIP1 X-ray structure, the residues preceding Lys<sup>-4</sup> do not diffract; they are unstructured and do not contribute to the binding [4]. One can conclude the short  $\beta$ 2- $\beta$ 3 loop of PDZ3 (approximately six residues) precludes significant interaction between the loop and C terminus of CRIP1. An active role of the  $\beta$ 2- $\beta$ 3 loop in ligand recognition has been reported for the PDZ2 domain from human tyrosine-phosphatase hPTP1E [8]. In the structure of PDZ2 of hPTP1E, an Asn residue in the middle of the  $\beta$ 2- $\beta$ 3 loop is proposed to hydrogen bond with the ligand, interacting with a Glu carboxylic acid in position -5 of the peptide. Here, a number of intermolecular NOEs are detected for Tyr<sup>-5</sup> placing the side chain in a gap formed by the end of the  $\beta$ 2 strand and the large  $\beta$ 2- $\beta$ 3 loop. Although few intermolecular NOEs are observed for the Lys<sup>-4</sup> side chain, the backbone carbonyl forms hydrogen bonds to the side chain amide of Asn<sup>85</sup>. In our previous study of the C terminus of the GluR6 subunit of kainate receptors [5], a similar perturbation of the Asn<sup>85</sup> side chain was observed, consistent with an interaction originated by the ligand backbone.

The lactam ring including Glu<sup>-1</sup>, Lys<sup>-3</sup>, and the  $\beta$ -Ala linker not only preserves the canonical binding of PDZ ligands, but by extending over the surface of the  $\beta$  sheet, actively contributes to the binding affinity. The side chains of both Glu<sup>-1</sup> and Lys<sup>-3</sup> are involved in a number of NOEs with residues of the  $\beta$ 2 and  $\beta$ 3 strands, namely Ser<sup>78</sup>, Ala<sup>80</sup>, Lys<sup>98</sup>, and Ile<sup>100</sup>. The lactam containing ring adopts a square-like conformation, with the fully extended side chains of Glu<sup>-1</sup> and Lys<sup>-3</sup> projecting perpendicularly to the  $\beta$ 2-strand and the  $\beta$ -Ala linker, connecting Glu<sup>-1</sup> and Lys<sup>-3</sup> and running antiparallel atop the  $\beta$ 3 strand of PDZ1. Given the sequence variation of this region within different PDZ domains, ligand/receptor

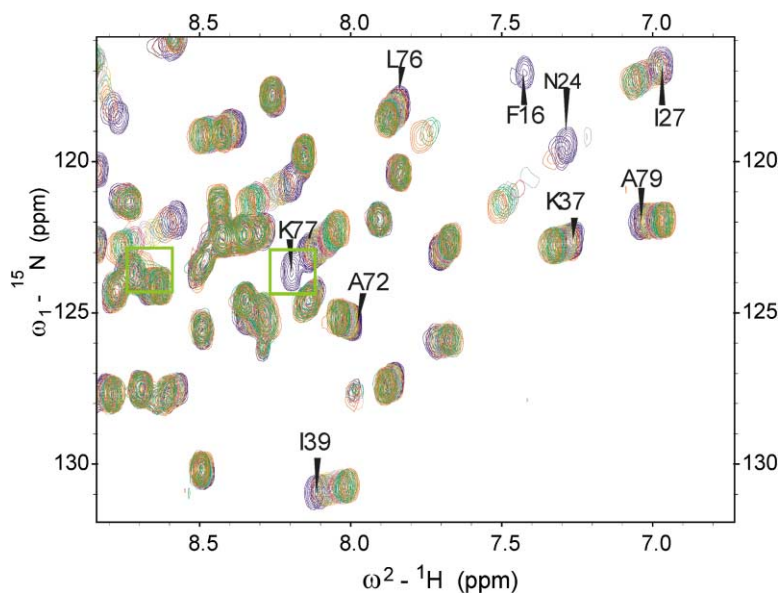


Figure 2. NMR-Based Ligand Binding

<sup>1</sup>H,<sup>15</sup>N HSQC NMR spectrum of the PDZ1 domain of PSD-95 during the titration of the ligand. Some of the amide resonances described in the text are denoted.

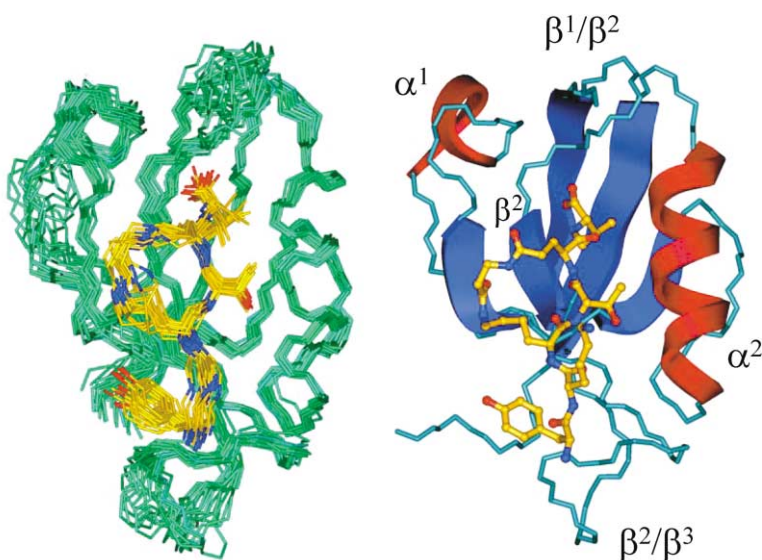


Figure 3. Ligand/PDZ1 Complex

Structure of the peptide/PDZ1 complex as determined by NMR. Left, a superposition (using the heavy backbone atoms of the PDZ1 domain) of 23 structures from the structure refinement calculations. Right, a ribbon representation of one structure, illustrating the mode of ligand binding and the lactam linker, extending over the  $\beta^2$  strand defining the canonical binding pocket.

interactions here may be targeted for enhanced PDZ specificity.

#### Biological Function Assays

We have previously shown that the association of the GluR6 subunit of the kainate receptor and PSD-95 is mediated through the C terminus of GluR6 and PDZ1 of PSD-95 [9]. To examine the activity of the cyclic peptide, the GluR6 and PSD-95 cDNAs are transfected into HEK293 cells, and after 24 hr, peptides are transduced into the cells using the bioporter reagent. In this assay, a 5- to 10-fold smaller quantity of the cyclic peptide was required to disrupt the interaction of GluR6 and PSD-95 versus a control peptide (containing the final 15 amino acids of the C terminus of GluR6). As illustrated in Figure 5, the cyclic peptide, at a concentration of 8  $\mu\text{g/ml}$ , is very efficient in competing against the C terminus of GluR6 for the PDZ1 domain, whereas 40  $\mu\text{g/ml}$  of control peptide was necessary to produce a similar disruption. The cyclic peptide also displays a more rapid onset of activity and, presumably because of reduced peptide enzymatic degradation, a much longer duration of biological function.

A similar response is observed in a cell-based assay. Previously, we found that PSD-95 promoted clustering of GluR6 kainate receptors when coexpressed in HEK293 cells [9]. Here, we have used this assay to examine the enhanced ability of the cyclic peptide to disrupt the GluR6/PSD-95 interaction. Compared to the linear control peptide, the cyclic peptide is found to disrupt the clustering of kainate receptors for extended periods of time. The linear form of the peptide displays a maximum inhibitory function of 5 hr, which steadily drops off and is completely abolished after 14 hr. In the same assay, we observe that the cyclic peptide displays appreciable inhibition of receptor clustering for 18 hr (Figure 6), consistent with enhanced enzymatic stability.

#### Significance

The shallow binding pocket of the canonical PDZ structure makes it an extremely challenging target for the

development of analogs with the desirable properties of high affinity and PDZ domain specificity. The novel macrocyclic cyclic peptide described here presents a method to address both of these issues. The cyclic peptide displays a 10-fold increase in binding affinity. As the NMR-based structural studies indicate, the lactam

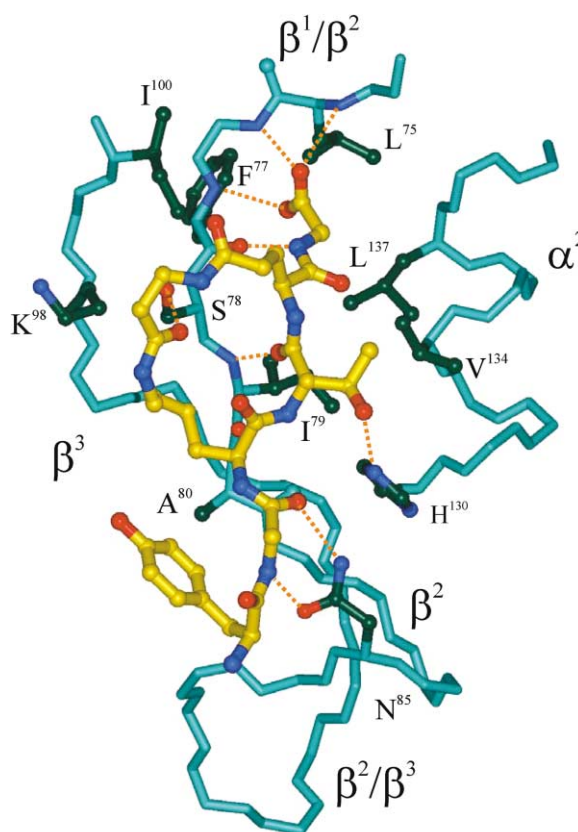
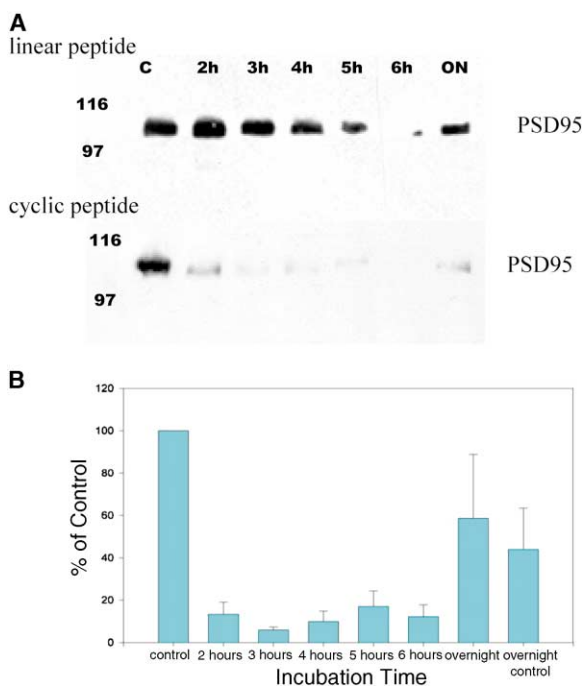


Figure 4. Specific Interactions of Cyclic Ligand with PDZ1

Expanded view of the peptide/PDZ1 complex, illustrating many of the residues involved in ligand binding (dark green).



**Figure 5. Inhibition of PSD-95/GluR6 Interaction**  
Time profile of the action of the cyclic peptide in disrupting the interaction between PSD-95-GluR6 subunit of the kainate receptor. A comparison of the cyclic peptide with the linear 15-amino acid peptide containing the C terminus of GluR6 to compete against the PSD-95/GluR6 association as measured by immunoprecipitation. Even overnight (14 hr), the cyclic peptide remains active.

ring system extends over the  $\beta 2$ -strand, interacting with a region of the PDZ domain with high sequence variability, providing a novel target for PDZ-domain specificity. The extended duration of bioactivity of the cyclic peptide is an important feature for the physiological characterization of the role of the GluR6/PDZ1 association, as well as further development of this molecular scaffold to target additional PDZ domains of PSD-95 as well as other PDZ containing proteins.

## Experimental Procedures

### Synthesis

The peptide was one of a series of novel macrocyclic peptides designed and prepared to function as conformationally constrained ligands for the PDZ domain [7]. Based upon the C-terminal sequence of CRIPT, this peptide possesses a bis-amide  $\beta$ -Ala bridge that links the  $P_{-1}$  and  $P_{-3}$  side chains. The peptide was synthesized using standard Fmoc solid phase peptide synthetic protocols, modified with orthogonal protecting groups for residues involved in the bridge formation. The final product was purified by reverse-phase HPLC and the mass confirmed by ESI-MS.

### NMR Spectroscopy

All NMR spectra of the complex were collected at 25°C on a Bruker Avance 600 MHz spectrometer equipped with a triple resonance probe and a triple axis gradient unit, while the spectra of the free peptide were collected at 25°C on a Bruker Avance 400 MHz equipped with a triple axis gradient unit. TSP was used as direct proton reference and as indirect  $^{13}\text{C}$  and  $^{15}\text{N}$  reference. The spectra were processed with NMRPipe and analyzed with Sparky 3. Distance, dihedral angles, and scalar coupling restraints were obtained from the NOESY spectra, from the chemical shift assignments, and from HNHA spectra, respectively, following published procedures [5]. Structures were calculated using the CNS program [10] employing the torsion angle simulated annealing protocol as described previously [5], resulting in 23 structures with no NOE violation greater than 0.3 Å, dihedral angle violation greater than 5°, and coupling constant violation greater than 1 Hz.

The conformation of the free peptide in solution was studied on a 1 mM sample dissolved in 600  $\mu\text{l}$  of  $\text{H}_2\text{O}$  (pH 4.5). The peptide resonances were assigned using DQF-COSY and TOCSY (mixing time 65 ms) experiments. The interproton distances were obtained from ROESY experiments employing a 280 ms mixing time and a 3.1 kHz spinlock field.

The NMR experiments of the PDZ1-peptide complex were performed on a 300  $\mu\text{l}$  solution containing 1 mM  $^{15}\text{N}/^{13}\text{C}$  enriched protein, 3 mM peptide, 10 mM phosphate buffer, and 150 mM NaCl (pH 6.8). The resonance assignment and measurement of intra- and intermolecular NOEs were obtained by HNCA, CBCA(CO)NH, HBHA (CO)NH, HCCH-TOCSY,  $^{15}\text{N}$ -NOESY-HSQC, and  $^{13}\text{C}$  NOESY-HSQC spectra following standard procedures [11, 12]. All of the backbone resonances were assigned, with the exception of the N- and C-terminal residues and the  $^{15}\text{N}$  resonances of the prolines. The HNHA spectra were employed to evaluate the coupling constants between the amide and the  $\text{H}_{\alpha}$  protons [13].

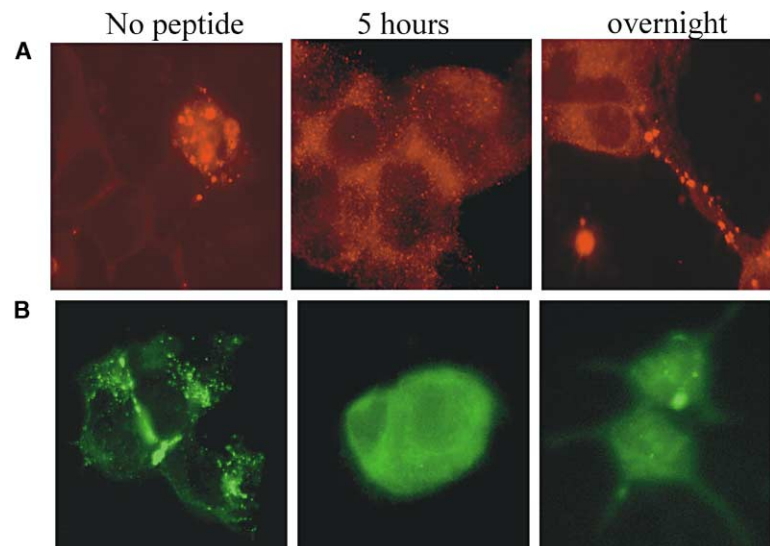


**Figure 6. Kainate Receptor Clustering Inhibition**

Staining of the GluR6 subunit of the kainate receptor in the presence of (A) the linear 15-amino acid peptide containing the C terminus of GluR6 and (B) the cyclic peptide. Both peptides are active in the disruption of the clustering of the kainate receptors, with the cyclic peptide still active even after 14 hr (overnight).

### Biological Function Assays

#### Microscopy

The interaction of the GluR6 subunit of the kainate receptor with PSD-95 was examined by the amount of clustering detected by microscopy. One 60 mm dish of HEK293 cells was transfected with GluR6GFP and PSD-95 cDNA constructs using Fugene 6 Transfection Reagent (Roche), then split onto poly-D-lysine coated coverslips. After 24–30 hr, the peptide was introduced via Bioporter (Sigma). At the appropriate time points, the coverslips were fixed with paraformaldehyde, rinsed with 1× PBS, and mounted onto slides for viewing.

#### Immunoblotting

In order to better quantify the effect of the peptide on the PSD-95/GluR6 interaction, a series of immunoprecipitations at differing time points were conducted. HEK293 cells were transfected with PSD-95 and myc-tagged GluR6 cDNA constructs. After 20–24 hr, the peptide was added (3 μg/ul of media) via the Bioporter reagent (Sigma) and incubated at 37°C. After the appropriate time point, the dishes were removed, carefully rinsed with DMEM and 1× TBS so as to not disrupt the cells, then homogenized in a 1× SALTERS buffer (50 mM Tris [pH 8.0], 150 mM NaCl, 1% NP40, 0.5% DOC, 0.1% SDS, 2 mM EDTA). The cells were then solubilized for 1 hr at 4°C and cleared by centrifugation at 14,000g for 30 min. The supernatant was extracted and then incubated overnight with 4 μg of *c-myc* primary antibody (Santa Cruz). Protein G sepharose beads (Amersham Biosciences) were added to the extract and incubated at 4°C for 1 hr. After a series of washes with SALTERS, standard 2× protein loading buffer containing 4 mM DTT was added, the samples were boiled for 5 min, and resolved on an 8% SDS-PAGE. Gels were then Western blotted, immunostained with α-PSD-95 monoclonal antibody (Upstate), and visualized with Supersignal West Pico chemiluminescent substrate (Pierce). The blots were analyzed using ImageJ (NIH) to calculate densitometry units and graphed with SigmaPlot (SPSS).

### Acknowledgments

This work was supported in part by grants from the National Institutes of Health, GM-63021 (M.R.S.), DA-15173 (D.F.M.), and RR-15578 (J.M. and D.F.M.).

Received: November 21, 2003

Revised: January 8, 2004

Accepted: January 8, 2004

Published: April 16, 2004

### References

1. Cho, K.O., Hunt, C.A., and Kennedy, M.B. (1992). The rat brain postsynaptic density fraction contains a homolog of the *Drosophila* discs-large tumor suppressor protein. *Neuron* 9, 929–942.
2. Kistner, U., Wenzel, B.M., Veh, R.W., Cases-Langhoff, C., Garner, A.M., Appeltauer, U., Voss, B., Gundelfinger, E.D., and Garner, C.C. (1993). SAP90, a rat presynaptic protein related to the product of the *Drosophila* tumor suppressor gene *dlg-A*. *J. Biol. Chem.* 268, 4580–4583.
3. Kuhlendahl, S., Spangenberg, O., Konrad, M., Kim, E., and Garner, C.C. (1998). Functional analysis of the guanylate kinase-like domain in the synapse-associated protein SAP97. *Eur. J. Biochem.* 252, 305–313.
4. Doyle, D.A., Lee, A., Lewis, J., Kim, E., Sheng, M., and MacKinnon, R. (1996). Crystal structures of a complexed and peptide-free membrane protein-binding domain: molecular basis of peptide recognition by PDZ. *Cell* 85, 1067–1076.
5. Piserchio, A., Pellegrini, M., Mehta, S., Blackman, S.M., Garcia, E.P., Marshall, J., and Mierke, D.F. (2002). The PDZ1 domain of SAP90. Characterization of structure and binding. *J. Biol. Chem.* 277, 6967–6973.
6. Tochio, H., Hung, F., Li, M., Brecht, D.S., and Zhang, M. (2000). Solution structure and backbone dynamics of the second PDZ domain of postsynaptic density-95. *J. Mol. Biol.* 295, 225–237.
7. Li, T., Saro, D., and Spaller, M.R. (2004). Thermodynamic profiling of conformationally constrained cyclic ligands for the PDZ domain. *Bioorg. Med. Chem. Lett.* 14, 1385–1388.
8. Kozlov, G., Banville, D., Gehring, K., and Ekiel, I. (2002). Solution structure of the PDZ2 domain from cytosolic human phosphatase hPTP1E complexed with a peptide reveals contribution of the beta2-beta3 loop to PDZ domain-ligand interactions. *J. Mol. Biol.* 320, 813–820.
9. Garcia, E.P., Mehta, S., Blair, L.A., Wells, D.G., Shang, J., Fukushima, T., Fallon, J.R., Garner, C.C., and Marshall, J. (1998). SAP90 binds and clusters kainate receptors causing incomplete desensitization. *Neuron* 21, 727–739.
10. Brunger, A.T., Adams, P.D., Clore, G.M., DeLano, W.L., Gros, P., Grosse-Kunstleve, R.W., Jiang, J.S., Kuszewski, J., Nilges, M., Pannu, N.S., et al. (1998). Crystallography & NMR system: A new software suite for macromolecular structure determination. *Acta Crystallogr. D Biol. Crystallogr.* 54, 905–921.
11. Clore, G.M., and Gronenborn, A.M. (1994). Young Investigator Award Lecture. Structures of larger proteins, protein-ligand and protein-DNA complexes by multidimensional heteronuclear NMR. *Protein Sci.* 3, 372–390.
12. Sattler, M., Schleucher, J., and Griesinger, C. (1999). Heteronuclear multidimensional NMR experiments for the structure determination of proteins in solution employing pulsed field gradients. *Prog. NMR Spec.* 34, 93–158.
13. Vuister, G.W., and Bax, A. (1994). Measurement of four-bond HN-H alpha J-couplings in staphylococcal nuclease. *J. Biomol. NMR* 4, 193–200.